Available online at www.sciencedirect.com
SCIENCE DIRECT®
International Journal of Heat and Mass Transfer 48 (2005) 4633–4639
International Journal of HEAT and MASS TRANSFER
www.elsevier.com/locate/ijhmt

The effect of thermodiffusion on the stability of a salinity gradient solar pond

Celestino Angeli [a], Erminia Leonardi [b,*]

[a] Dipartimento di Chimica, Università di Ferrara, Via Borsari 46, I-44100 Ferrara, Italy
[b] CRS4, Center for Advanced Studies, Research and Development in Sardinia, Parco Scientifico e Tecnologico, Polaris, Edificio 1, 09010 Pula, CA, Italy

Received 13 September 2004

Dedicated to Lorenzo

Abstract

A one-dimensional mathematical model is used for the study of the NaCl diffusion in a salinity-gradient solar pond. The model takes into account the effect of the thermodiffusion, or Soret effect, and also the possibility of injection of concentrated brine at the bottom of the salinity-gradient zone of the solar pond. The model results show that the thermodiffusion moves in the same direction of the molecular diffusion process, thus contributing to destabilize the salinity-gradient layer. This effect can be a significant contribution to the salt diffusion (over 10%), when the temperature gradient and salt concentration are high, like at the bottom of the salinity-gradient zone.

Keywords: Solar pond; Thermodiffusion; Soret effect; Salt diffusion; Finite difference 1D numerical methods

1. Introduction

The principle of operation of a solar pond is quite simple, being a basin several meters deep, filled with stratified brine varying in concentration from near saturation, at the bottom, to approximately the sea water concentration at the surface. About 25% of the solar radiation incident at the surface penetrates to the bottom of the pond and it is absorbed there, causing the adjacent brine to heat up. The heat is stored in the bottom part of the solar pond because convective motions bringing the hot water to the surface are hindered by the salinity gradient which therefore acts as an insulator.

Therefore, in practice, a typical solar pond consists of three distinct regions: two convective regions, one at the top (upper convective zone, UCZ) and one at the bottom (lower convective zone, LCZ), separated by a quiescent nonconvecting region (nonconvective zone, NCZ) characterized by strong temperature and salinity gradients (see Fig. 1).

Although the diffusion flux tends to homogenize the system, the maintenance of the salinity profile in the solar pond can be obtained by addition of salt, or concentrated brine at the LCZ and fresh water, or low salinity brine flushing, at the UCZ, which results in a rising velocity of the NCZ (rising solar pond [1,2]).

* Corresponding author. Tel.: +39 070 9250328; fax: +39 070 9250216.
E-mail address: ermy@crs4.it (E. Leonardi).

0017-9310/$ - see front matter © 2005 Elsevier Ltd. All rights reserved.
doi:10.1016/j.ijheatmasstransfer.2005.05.021

Nomenclature

c	salt concentration, kg m^{-3}
c_{inj}	concentration of the injected brine, kg m^{-3}
D	salt diffusivity, m^2 s^{-1}
$\vec{J}$	total mass flux, kg m^{-2} s^{-1}
$\vec{J}_D$	diffusive mass flux, kg m^{-2} s^{-1}
$\vec{J}_S$	thermodiffusive mass flux, kg m^{-2} s^{-1}
k	thermal conductivity, W m^{-1} °C^{-1}
LCZ	lower convective zone
w_1	salt weight fraction, dimensionless
NCZ	nonconvective zone
$\dot{q}$	heat generated per unit time and volume, W m^{-3}
S	salinity, %
s_T	Soret coefficient, °C^{-1}
T	temperature, °C
T_L	temperature in the LCZ, °C
T_U	temperature in the UCZ, °C
UCZ	upper convective zone
$\vec{v}$	velocity of the injected brine, m s^{-1}
W	solar power density, W m^{-2}
z	solar pond height, measured from the bottom ($z = H - Z$), m

Greek symbol

ρ	density, kg m^{-3}

Superscripts

$\vec{x}$	vector variable
$\dot{x}$	time derivative

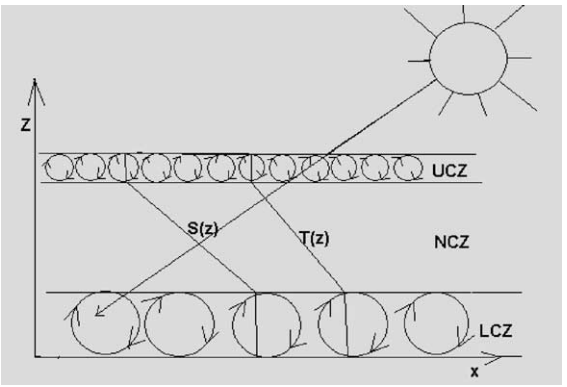

Fig. 1. Schematic of a solar pond.

In a previous paper [3] (hereafter called paper I) a one dimensional model based on a finite difference scheme was used to describe the salt diffusion within a solar pond. In the present work, the analysis of the behaviour of the solar pond has been extended by considering also the effect of the thermodiffusion on the global stability of the system. The rest of this paper is organized as follows: in Section 2, we briefly describe the phenomenon of the thermodiffusion; in Section 3, the mathematical scheme used to model the thermodiffusion within the solar pond is presented; in Section 4, the results of the model are shown and the effect of the thermodiffusion on the stability of the system is discussed.

2. The phenomenon of the thermodiffusion

The thermodiffusion, or Ludwig–Soret effect, is the separation of the components of a liquid mixture induced by temperature gradients. The migration of atoms and molecules as a consequence of a temperature gradient was first reported by Ludwig [4] when studying sodium-sulphate solutions in 1856. Later, in 1879, Soret [5] observed the same effect in other electrolyte solutions.

Although there are numerous examples for the technological significance of the thermodiffusion [6,7], there is still no satisfactory theory to explain the phenomenon. The fact that this effect happens does not itself need an explanation: once the temperature difference takes a multicomponent system away from equilibrium and breaks translational symmetry, there is no reason why the ratio of concentrations should stay constant. Nevertheless, the thermodiffusion continues to be *the only hydrodynamic transport mechanism that lacks a simple physical explanation* [6]. The Soret coefficient strongly varies with the nature of the components of the mixture and with their concentration. In fact it appears to be sensitive to the details of the molecular interaction potentials and cannot easily be measured experimentally and predicted theoretically [8,9]. However, recent developments of nonequilibrium molecular dynamics methods has allowed the study of thermodiffusion at microscopic level [10–13], and the Soret coefficients of various mixtures have been calculated.

2.1. The thermodiffusion in the solar pond

There are few data about thermodiffusion in solar ponds. Rothmeyer [14] calculated salt fluxes for the University of New Mexico solar pond and found that the flux due to the Soret effect was only about 4% of the diffusive flux during the winter but rose to almost 30% in the summer when the temperature gradients were stron-

ger. However, his estimations comes from a rough analysis of the various terms of the diffusion equation, without any solution of differential equations.

In this work, we use the empirical formulation reported by Sherman [15] to describe the thermodiffusion contribution to the salt diffusion within a solar pond. Moreover, we also consider the injection of concentrated brine from the bottom of the solar pond, thus introducing a new mass flux term, $v \times c$, in the diffusion equation.

3. The mathematical model

The formalism reported in this section closely resembles the one presented in paper I to which the reader is referred for the details.

By taking into account the molecular diffusion, the thermodiffusion, and the rising velocity of the NCZ due to the injection of concentrated brine from the bottom of the solar pond, the principle of mass conservation for the solute gives an equation of the form

$$\begin{aligned}\frac{\partial w_1}{\partial t} &= -\vec{\nabla}\cdot\vec{J} = -\vec{\nabla}\cdot(\vec{J}_{\mathrm{D}} + \vec{J}_{\mathrm{S}} + \vec{v}c) \\ &= -\vec{\nabla}\cdot(-D\rho\vec{\nabla}w_1 - D\rho s_T w_1(1-w_1)\vec{\nabla}T + \vec{v}\rho w_1)\end{aligned} \tag{1}$$

where $\vec{J}$ is the total mass flux, $\vec{J}_{\mathrm{D}}$ is the diffusive mass flux, $\vec{J}_{\mathrm{S}}$ is the mass flux contribution due to the thermodiffusion, $\vec{v}$ is the rising velocity of the NCZ, positive upward and constant with respect to time and space, ρ is the density, w_1 is the weight fraction of the salt, D is the diffusivity, and s_T is the Soret coefficient which is an increasing function of the temperature. The form here used for $\vec{J}_{\mathrm{S}}$ has a phenomenological derivation and contains the product of the weight fractions of the salt (w_1) and of the water ($1-w_1$), given that its expression should be symmetrical with respect to both components [16].

Being the temperature of the NCZ a function of the depth, also the Soret coefficient is in general a function of z. Moreover, being $w_1 = \frac{c}{\rho}$, where c is the salt concentration, Eq. (1) can be written as follows:

$$\frac{\partial c}{\partial t} = -\vec{\nabla}\cdot\left\{-D\vec{\nabla}c - Ds_T c\left(1-\frac{c}{\rho}\right)\vec{\nabla}T + \vec{v}c\right\} \tag{2}$$

Eq. (2) can be solved numerically, using a finite difference scheme and a second-order accurate in time Crank–Nicholson method [17]. The concentration $c(z,t)$ is computed on a regular grid of points in z ($\{z_1, z_2, \ldots, z_{n_z}\}, z_{i+1} - z_i = \Delta z$) and t ($\{t_1, t_2, \ldots, t_{n_t}\}$, $t_{i+1} - t_i = \Delta t$). For the sake of simplicity we used the compact formalism $c_{i,j}$ for $c(z_i, t_j)$. By using this notation, Eq. (2) can be discretized in the following way:

$$\begin{aligned}\frac{c_{i,j}-c_{i,j-1}}{\Delta t} &= \frac{1}{2(\Delta z)^2}\{D_{i+\frac{1}{2}}[(c_{i+1,j}-c_{i,j}) + (c_{i+1,j-1}-c_{i,j-1})] \\ &\quad + D_{i-\frac{1}{2}}[(c_{i-1,j}-c_{i,j}) + (c_{i-1,j-1}-c_{i,j-1})]\} \\ &\quad + \frac{1}{2\Delta z}\left[D_{i+1}s_{T_{i+1}}c_{i+1,j-1}\left(1-\frac{c_{1+1,j-1}}{\rho_{i+1,j-1}}\right)\left(\frac{\partial T}{\partial z}\right)_{i+1}\right. \\ &\quad \left. - D_{i-1}s_{T_{i-1}}c_{i-1,j-1}\left(1-\frac{c_{1-1,j-1}}{\rho_{i-1,j-1}}\right)\left(\frac{\partial T}{\partial z}\right)_{i-1}\right] \\ &\quad - v\frac{(c_{i+1,j}-c_{i-1,j}) + (c_{i+1,j-1}-c_{i-1,j-1})}{4\Delta z}\end{aligned} \tag{3}$$

where

$$D_{i+\frac{1}{2}} = \frac{D(z_{i+1}) + D(z_i)}{2} \tag{4}$$

$$D_{i-\frac{1}{2}} = \frac{D(z_{i-1}) + D(z_i)}{2} \tag{5}$$

Eq. (3) can be rewritten in the form of a system of linear equations (one set for each time t_j):

$$\begin{aligned}&(\alpha_{i+\frac{1}{2}} - \beta)c_{i+1,j} - (1 + \alpha_{i+\frac{1}{2}} + \alpha_{i-\frac{1}{2}})c_{i,j} + (\beta + \alpha_{i-\frac{1}{2}})c_{i-1,j} \\ &\quad = B_{i,j}\end{aligned} \tag{6}$$

where

$$\beta = \frac{v\Delta t}{4\Delta z} \tag{7}$$

$$\alpha_{i+\frac{1}{2}} = \frac{D_{i+\frac{1}{2}}\Delta t}{2(\Delta z)^2} \tag{8}$$

$$\alpha_{i-\frac{1}{2}} = \frac{D_{i-\frac{1}{2}}\Delta t}{2(\Delta z)^2} \tag{9}$$

and

$$\begin{aligned}B_{i,j} &= \beta(c_{i+1,j-1} - c_{i-1,j-1}) - \alpha_{i+\frac{1}{2}}(c_{i+1,j-1} - c_{i,j-1}) \\ &\quad - \alpha_{i-\frac{1}{2}}(c_{i-1,j-1} - c_{i,j-1}) - c_{i,j-1} \\ &\quad - \frac{t\Delta}{2\Delta z}\left[D_{i+1}s_{T_{i+1}}c_{i+1,j-1}\left(1-\frac{c_{1+1,j-1}}{\rho_{i+1,j-1}}\right)\left(\frac{\partial T}{\partial z}\right)_{i+1}\right. \\ &\quad \left. - D_{i-1}s_{T_{i-1}}c_{i-1,j-1}\left(1-\frac{c_{1-1,j-1}}{\rho_{i-1,j-1}}\right)\left(\frac{\partial T}{\partial z}\right)_{i-1}\right]\end{aligned} \tag{10}$$

We note that thermodiffusion, being a small contribution to the Fick salt diffusion [14], can be considered a very slow process. Therefore we can approximate its magnitude at the time step j using the concentration of the step $j-1$. Thus, in the system of linear equation (6) its contribution appears on the right-hand side.

The system of linear equation (6) can be written in the matrix form

$$\mathbf{A}\mathbf{C}_j = \mathbf{B}_j \quad \forall j = 2, n_t \tag{11}$$

and it can be easily solved, once the initial ($c_{i,0}$, for all i) and boundary conditions are imposed, by using

standard mathematical libraries (as for instance the LAPACK ones [18]).

4. Discussion of the simulation results

In paper I we have studied the salt diffusion process within a solar pond, neglecting the thermodiffusion effect. Here, we present the simulation results when thermodiffusion is also considered and we discuss the time-scale of the overall salt diffusion process.

The diffusivity coefficient is a function of the temperature and salinity [3], and it is obtained by a least square fit to the International Critical Tables for a range of temperature between 5 °C and 100 °C and for a salinity range between 0% and 20% [19]:

$$D_{i,j} = (8.16 + 0.255T_i + 0.00254T_i^2 - 0.28S_{i,j} + 0.0147S_{i,j}^2) \times 10^{-10} \quad (12)$$

where S is the salinity in weight percent ($S = c/\rho \times 100$) and $D_{i,j}$ is in $m^2\,s^{-1}$.

The density, $\rho_{i,j}$ (kg m^{-3}), at any point z_i,t_j, is a function of the temperature T and of the salinity S(g kg^{-1}). In the case of a NaCl aqueous solution ρ is given by [20]:

$$\rho(z,t) = 1000 \times \left\{1 - \frac{T+a}{b \times (T+c)} \times (T-d)^2\right\} + e(T) \times S + f(T) \times S^{\frac{3}{2}} + g \times S^2 \quad (13)$$

where $a = 288.9414$, $b = 508929.2$, $c = 68.12963$, $d = 3.9863$, $g = 4.8314 \times 10^{-4}$ and

$$e(T) = 8.24493 \times 10^{-1} - 4.0899 \times 10^{-3} \times T + 7.6438 \times 10^{-5} \times T^2 - 8.2467 \times 10^{-7} \times T^3 + 5.3675 \times 10^{-9} \times T^4$$

$$f(T) = -5.724 \times 10^{-3} + 1.0227 \times 10^{-4} \times T - 1.6546 \times 10^{-6} \times T^2$$

The Soret coefficient is extracted from the measurements of Caldwell [21], for a 0.5 normal NaCl aqueous solution and in the range of temperature between 0 °C and 50 °C. The overall curve in the range between 0 °C and 50 °C has been fitted with a cubic polynomial function: this function has been also used between 50 °C and 100 °C, that is outside the fitting interval, where it shows an almost linear behaviour, as shown in Fig. 2.

We choose the thickness of the UCZ, NCZ and LCZ according to those of the El Paso's solar pond [22], which are 0.7, 1.2 and 1.35 m respectively. Also, the temperatures of the UCZ and NCZ, and the monthly averaged solar power density are chosen according to the major climatic and geological conditions at El Paso [22], and are reported in Figs. 3 and 4.

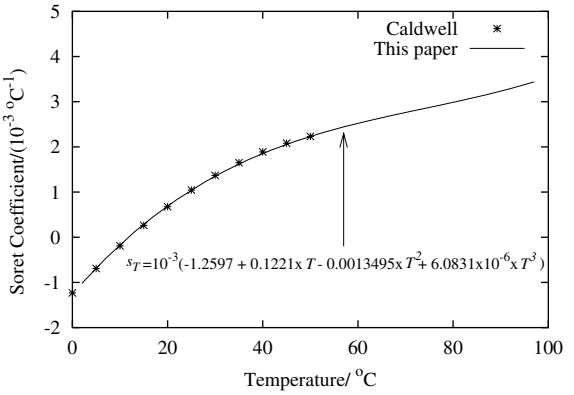

Fig. 2. Soret coefficient, s_T, as a function of the temperature for a water solution of NaCl 0.5 N. Caldwell's function up to 50 °C is $s_T = 10^{-3}(-1.2321 + 0.1128 \times T - 0.00087 \times T^2)$.

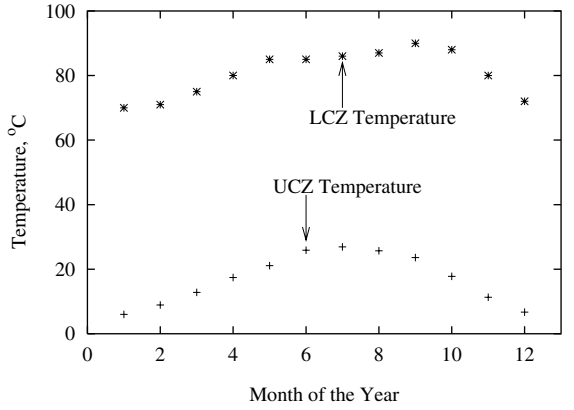

Fig. 3. UCZ and LCZ temperature development at the El Paso's solar pond.

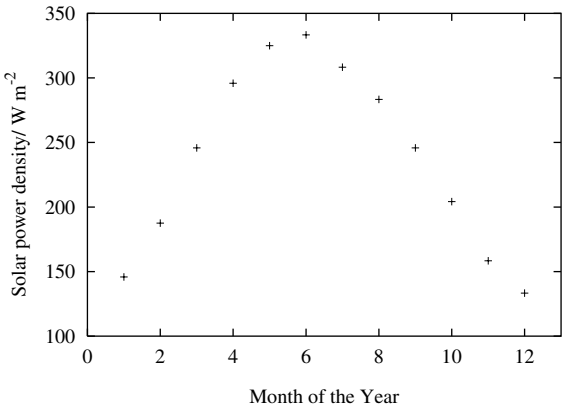

Fig. 4. Solar power density monthly averaged at the El Paso's solar pond.

The temperature profile within the NCZ is computed by using the steady-state conduction heat equation:

$$\dot{q} + \frac{\partial}{\partial Z}\left(k\frac{\partial T}{\partial Z}\right) = 0 \tag{14}$$

where k is the thermal conductivity, $\dot{q}$ is the solar energy absorbed from the water per unit of time and per unit of volume:

$$\dot{q} = -\frac{\partial W}{\partial Z} \tag{15}$$

where $W(Z)$ is the solar power density at the depth Z measured from the water surface.

Moreover, the initial salt concentration is a linear function of the depth from 40 kg m^{-3} at the boundary between the UCZ and the NCZ to 200 kg m^{-3} at the boundary between the NCZ and the LCZ. The salt diffusion is computed by discretization of the computational domain with $\Delta z = 0.01$ m, and $\Delta t = 1.0$ day.

The contribution of the thermodiffusion to the total diffusion process has been calculated considering the effect of the rising velocity of the injected brine.

The result of the case with zero rising velocity is shown in Fig. 5, after 1 year of simulation. In particular, the fluxes during the summer and the winter are plotted.

The fluxes in the UCZ and LCZ are not indicated in the figure because the temperature and concentration gradients are both zero in these regions. Because of the higher temperature gradient during the summer, the Soret flux is also higher during that season. As shown in Fig. 6, the percentage of the ratio J_S/J_D is always below 15% both in summer and winter, although, close to the LCZ, it is greater in summer and close to the UCZ it is greater in winter (the annual averaged percentage over the full NCZ spatial domain), is about 9%). In Fig. 7 the percentage of the ratio J_S/J_T, with $J_T = J_S + J_D$ the total flux, under summer and winter solar pond conditions is also shown. In this case the overall annual averaged percentage is about 8%.

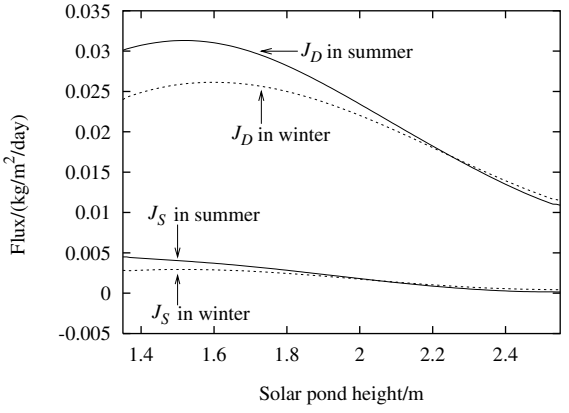

Fig. 5. Comparison between the diffusion flux, J_D, and the Soret flux, J_S, in the salinity-gradient layer, in summer and winter.

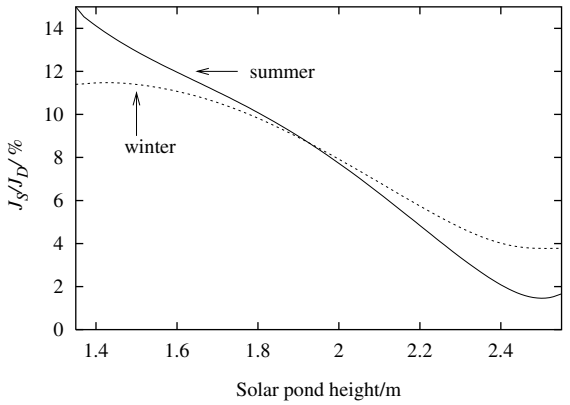

Fig. 6. Percentage of the Soret to diffusive flux ratio in the salinity-gradient layer during the summer and the winter, after one year.

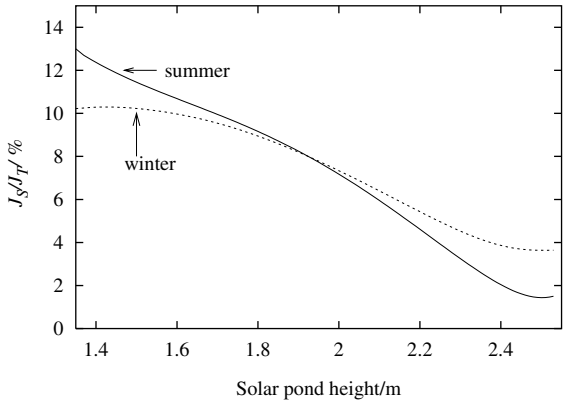

Fig. 7. Percentage of the Soret to the total flux ratio in the salinity-gradient layer during the summer and the winter, after one year.

After 30 years the simulation results (see Fig. 8) show that the system has reached a pseudo steady-state (there are seasonal variations of the temperatures, and therefore, the coefficients s_T and D show a periodic behaviour with time), which is characterized by a small concentration gradient (a slope of 8.41 kg m^{-4}), whose direction is opposite to the initial one, as attained from the sign of the Soret coefficient. After this simulation time the solar pond structure no longer exists: these results are here reported in order to show the effect of the thermodiffusion on the steady-state in absence of convective motions. From Fig. 7 one notes that the thermodiffusion destabilizes the salinity gradient, inducing the salt to migrate from the hot region toward the cold one, and thus destroying the salinity gradient.

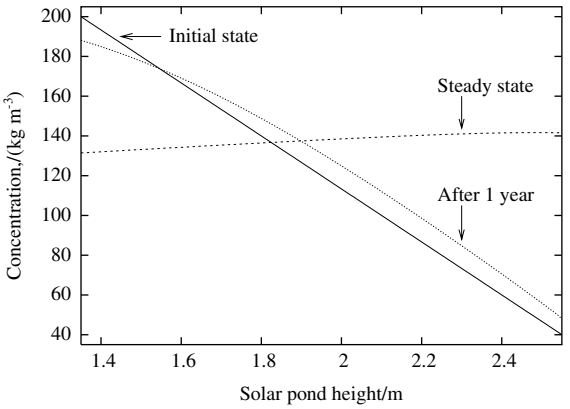

Fig. 8. Salt concentration profiles: initial state, after one year and steady-state (after 30 years).

If concentrated brine (we have chosen $C_{inj} = 300\ kg\ m^{-3}$) is injected at the boundary of the NCZ with the LCZ, while a constant concentration is maintained at the top ($c = 40\ kg\ m^{-3}$), the concentration gradient reduction is slower in time and the effect of the thermodiffusion on the total flux (see Eq. (1)) is reduced. Such effects are shown in Figs. 9 and 10, where the results after 1 year are plotted. In particular, Fig. 9 shows the development of the concentration profile with and without the injection of concentrated brine, with c_{inj} and v chosen similar to those of Alagao [2] ($c_{inj} = 300\ kg\ m^{-3}$, $v = 3.0^{-4}\ m\ s^{-1}$). Fig. 10 compares the annual averaged percentage of the Soret flux to the total flux, at different values of the injection velocity, showing that, for rising solar pond, the thermodiffusion can be considered a secondary effect, its contribution being of few percents, and, therefore, it can be neglected in the study of the salt diffusion.

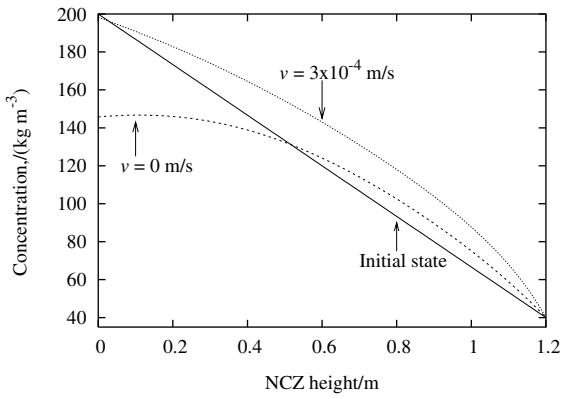

Fig. 9. Comparison of salt concentration profiles after one year, with and without injection of concentrated brine. $c_{inj} = 300\ kg\ m^{-3}$, $v = 3.0 \times 10^{-4}\ m\ s^{-1}$. The initial concentration is also plotted.

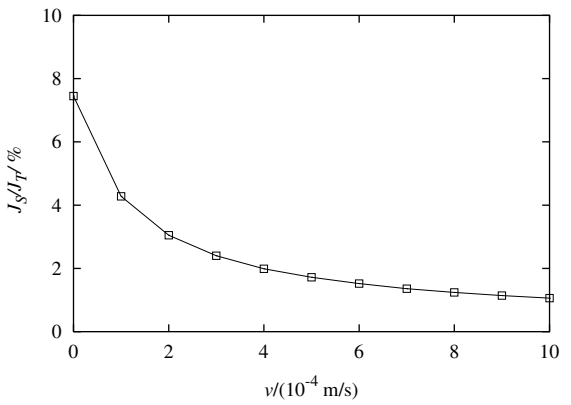

Fig. 10. Annual averaged percentage of the Soret to total flux ratio after one year at different values of velocity of injection of concentrated brine ($c_{inj} = 300\ kg\ m^{-3}$).

5. Conclusions

In this work, we have introduced the thermodiffusion effect into the salt diffusion equation, and solved numerically the 1D mathematical model by using the finite difference method. The solar pond has been dimensioned as the one operating at El Paso (Texas) [22]. Also, the seasonal fluctuations of the UCZ and LCZ temperatures have been assumed according with those measured at El Paso. The results of the model show that the thermodiffusion can reaches annual averaged percentage of the total flux close to 10%, with picks of about 15% in summer, and at the bottom of the NCZ. The injection of concentrated brine, necessary to maintain the salinity-gradient stable with the time, generates an additional flux which globally reduces the thermodiffusion contribution, the annual average of which becomes of the order of few percents.

Acknowledgements

The authors thank Bruno D'Aguanno for useful discussions and suggestions. This work has been carried out with the financial support of the "Regione Autonoma della Sardegna".

References

[1] H. Weinberger, The physics of solar pond, Solar Energy 8 (1964) 45.
[2] F.B. Alagao, Simulation of the transient behavior of a closed-cycle salt-gradient solar pond, Solar Energy 5 (1996) 245.
[3] C. Angeli, E. Leonardi, A one-dimensional numerical study of the salt diffusion in a salinity gradient solar pond, Int. J. Heat Mass Transfer 47 (2004) 1.

[4] C. Ludwig, S.K. Pressus, Akad. Wiss. 20 (1856) 539.
[5] C. Soret, Arch. Geneve 3 (1879) 48.
[6] J. Kincaid, B. Hafskjøld, Thermal diffusion factors for the Lennard–Jones spline system, Mol. Phys. 82 (1994) 1099.
[7] B. Hafskjøld, S. Ratkje, Coupled transport of heat and mass: theory and applications, in: J.S. Shiner (Ed.), Entropy and Entropy Generation, Kluwer Academic, Dordrecht, 1996, pp. 197–219.
[8] J.L. Lin, W.L. Taylor, W.M. Rutherford, J. Millat, in: W.A. Wakeman, A. Nagashima, J.V. Sengers (Eds.), Measurement of the Transport Properties of Fluids, Blackwell Scientific, Oxford, 1991, p. 321.
[9] D. Longree, J.C. Legros, G. Thomaes, Measured Soret coefficients for simple liquefied gas mixtures at low temperatures, J. Phys. Chem. 84 (1980) 3480.
[10] T. Ikeshoji, B. Hafskjøld, Non-equilibrium molecular dynamics calculations of heat conduction in liquid and through liquid–gas interface, Mol. Phys. 81 (1994) 251.
[11] F. Müller-Plathe, A simple nonequilibrium molecular dynamics method for calculating the thermal conductivity, J. Chem. Phys. 106 (1997) 6082.
[12] D. Reith, F. Müller-Plathe, On the nature of thermal diffusion in binary Lennard–Jones liquids, J. Chem. Phys. 112 (1999) 2436.
[13] P. Bordat, D. Reith, F. Müller-Plathe, The influence of interaction details on the thermal diffusion in binary Lennard–Jones liquids, J. Chem. Phys. 115 (2001) 8978.
[14] M.K. Rothmeyer, Saturated solar pond—modified equations and results of a laboratory experiment. Master's Thesis. University of New Mexico, 1976.
[15] B.S. Sherman, Modeling and control of a solar pond, Ph.D. Thesis, The University of Western Australia, 1989.
[16] H.J.V. Tyrrell, Diffusion and Heat Flow in Liquids, Butterworths, London, 1961.
[17] Numerical Recipes in FORTRAN 77: The Art of Scientific Computing, Cambridge University Press, 1992, pp. 838–842, ISBN 0-521-43064-X.
[18] E. Anderson, Z. Bai, C. Bischof, S. Blackford, J. Demmel, J. Dongarra, J. Du Croz, A. Greenbaum, S. Hammarli, A. McKenney, D. Sorensen, LAPACK Users' Guide, Third ed., Society for Industrial and Applied Mathematics, Philadelphia, PA, 1999, ISBN 0-89871-447-8.
[19] M. Giestas, A. Joyce, H. Pina, The influence of non-constant diffusivities on solar ponds stability, Int. J. Heat Mass Transfer 18 (1997) 4379.
[20] S.C. McCutcheon, J.L. Martin, T.O. Barnwell Jr., Water Quality in Maidment in Handbook of Hydrology, McGraw-Hill, New York, NY, 1993, p. 11.3.
[21] D. Caldwell, Deep Sea Res. 20 (1973) 1029.
[22] H. Lu, J.C. Walton, A.H.P. Swift, Desalination coupled with salinity-gradient solar ponds, Desalination 136 (2001) 13.